A SILICON NITRIDE OPTOMECHANICAL OSCILLATOR WITH ZERO FLICKER NOISE

S. Tallur, S. Sridaran and S.A. Bhave
OxideMEMS Laboratory, Cornell University, Ithaca, NY – USA

ABSTRACT

We present an integrated chip-scale Radiation-Pressure driven Opto-Mechanical Oscillator (RP-OMO) in silicon nitride with excellent close-to-carrier phase noise. We illustrate a process to micro-fabricate opto-mechanical resonators, waveguides and grating couplers in silicon nitride and demonstrate an RP-OMO operating at 41.95MHz, with phase noise of -85dBc/Hz at 1kHz offset. The phase noise does not show $1/f^3$ or other higher order slopes all the way down to 10Hz offset from carrier. Using a lower optical quality factor resonance, we demonstrate improvement of 6dB in phase noise.

INTRODUCTION

Overview of chip-scale oscillators

Quartz oscillators in tens of MHz range offer superior far-from-carrier phase noise, but have high flicker noise. Recent progress in MEMS based oscillators has gained a lot of attention owing to their potential to replace quartz crystals as reference oscillators. Chip scale MEMS oscillators spanning various transduction schemes have been shown – capacitive electrostatic [1, 2], piezoelectric [3] and piezoresistive [4, 5]. Barring [4], the other oscillators are not self-sustained and need a feedback amplifier. The amplifier's flicker noise shows up as $1/f^3$ noise for close-to-carrier offsets thereby degrading long term stability. Communication with authors [4, 5] suggests the self-oscillations have large jitter.

Review of radiation pressure in microcavities

Recent advances in photonics have enabled co-design of mechanical and optical resonances in the same device. Coupling of high quality factor (Q) mechanical modes of these microcavities to its optical modes has enabled interesting experiments in cavity optomechanics [6]. A notable contribution that has come out of this area of research is the manifestation of parametric instability in such resonators, resulting in mechanical amplification and thereby oscillation of the mechanical mode driven purely by radiation pressure (RP) of light.

RP driven oscillations have been extensively studied [6] and such oscillations have been observed by various teams [6, 7]. The coupling between the mechanical and optical modes of the cavity can be expressed via a coupled differential equation system [6]

$$\frac{da}{dt} = i\Delta(r)a - \left(\frac{1}{\tau_0} + \frac{1}{\tau_{ex}}\right)a + i\sqrt{\frac{1}{\tau_{ex}}}s \qquad (1)$$

$$\frac{d^2r}{dt^2} + \frac{\Omega_{mech}}{2Q_{mech}}\frac{dr}{dt} + \Omega_{mech}^2 = \frac{F_{RP}(t)}{m_{eff}} + \frac{F_L(t)}{m_{eff}} \qquad (2)$$

Here, a denotes the field circulating inside the cavity and s denotes the launched pump field, r denotes the amplitude of radial displacement of the microring cavity, and $\Delta(r)$ denotes the optical detuning that describes the coupling of equation (1) to (2). The detuning can be expressed as a function of the change in radius as $\Delta(r) = \Delta_0 + \lambda_0/R$, where Δ_0 is the detuning of the laser wavelength from the cavity resonant wavelength λ_0 and R is the radius of the micro-ring.

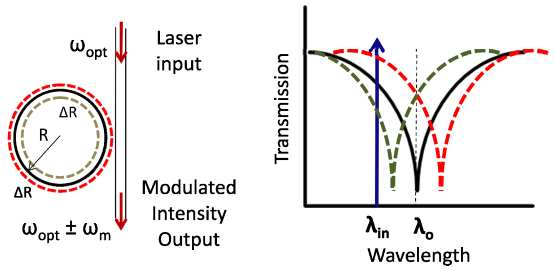

Figure 1: Illustration of shift in detuning with radial motion of the microring resonator periphery

At an intuitive level, this excitation process can be understood as follows. Consider a micro-ring optomechanical resonator evanescently coupled to a waveguide as shown in Figure 1. Assuming first that the optical pump laser wavelength is detuned from the cavity optical resonance wavelength, the circulating photons inside the cavity exert a radiation pressure force on the cavity. This force can be expressed as in equation (3), where n_{eff} is the effective refractive index for the optical mode in the cavity, F is the finesse, P_{circ} is the power circulating inside the cavity and P_{in} is the input laser power in the waveguide. The finesse is directly proportional to the optical quality factor and inversely proportional to the radius of the ring.

$$F_{RP} = \frac{2\pi n_{eff}}{c}P_{circ} = \frac{2n_{eff}F}{c}P_{in} \qquad (3)$$

The force induces deformation of the cavity and changes the optical resonant wavelength of the microcavity through a change in the optical path length. An increase in radius thus lowers the coupled optical pump power and hence the radiation pressure force. Such a phase relationship between optical pressure and microcavity deformation results in net power transfer from the optical pump laser to the mechanical mode. This transfer manifests itself mathematically as a mechanical gain, for the mechanical oscillations. Beyond a corresponding threshold optical power, the amplification rate exceeds the intrinsic mechanical damping rate and the circulating light inside the cavity sets up self-sustained mechanical oscillations. Interaction of the vibrating resonator with photons inside the cavity results in amplitude modulation of the pump laser light at the output of the resonator. This imprinting of the mechanical

oscillations on the laser light is converted into RF output power at the photodetector.

Prior art in RP-OMOs

RP-OMOs based on strong coupling between high-Q optical and mechanical modes of a microtoroid resonator have been demonstrated before [6, 7]. However making this device requires an unconventional post-fabrication CO_2 laser reflow step. The phase noise numbers reported [7] are far worse than those reported for CMOS oscillators in similar frequency ranges. The phase noise also shows higher order slopes at close to carrier frequencies that are unexplained but are often attributed to environmental noise. Theoretical analysis for OMOs [7, 8] indicates that these problems can be overcome by having a robust device with high mechanical and optical quality factors. Silicon nitride is a promising material for such an application owing to its high optical and mechanical quality factors. Being CMOS compatible, we can design resonators in silicon nitride using MEMS based processes.

Chip-scale opto-mechanical resonators in silicon nitride with integrated waveguides have been shown [9]; however no self-oscillations have been reported. We present a fabrication process to design released opto-mechanical resonators, grating couplers and integrated waveguides in silicon nitride. The next section describes the device design and the fabrication process.

DEVICE DESIGN

Device design

We choose a ring geometry for the microresonator owing to its high optical Q. The ring is designed to be wide (6µm) and with a large outer radius (40µm).

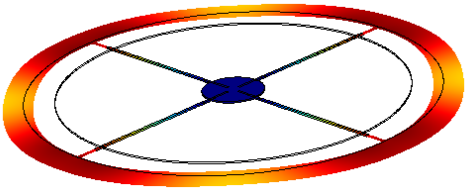

Figure 2: Simulated fundamental radial expansion mode shape for the ring resonator (radius 40µm, 6µm wide, 500nm wide spokes) at 41.1MHz. Deformed geometry for the expanded ring is illustrated here.

We design grating couplers to couple light into the waveguide. The waveguide width at the grating couplers is 15µm and it is tapered down to 800nm close to the resonator. The grating couplers were simulated in Lumerical Solutions FDTD and are designed to be broadband and have maximum transmission at 1550nm for light incident at an angle of 20° to the vertical. The ring resonator has a fundamental radial expansion mode at 41.1MHz as estimated from FEM simulations performed in COMSOL, as shown in Figure 2.

Process flow

Figure 3 illustrates the devised process flow schematically. We start with silicon wafers that have 4µm SiO_2 thermally grown and deposit 300nm Si_3N_4 using low pressure chemical vapor deposition (LPCVD). The devices are defined using electron beam lithography. The pattern is then etched into the nitride device layer in a CHF_3/O_2 reactive ion etch (RIE) step. We then deposit SiO_2 cladding using a plasma enhanced chemical vapor deposition (PECVD) system, to clad the gratings and waveguide with oxide. This is done to reduce losses at the grating couplers (simulated -10dB per coupler without cladding; -6dB per coupler with cladding). A second mask is then used to pattern release windows near the resonator using contact photolithography. This is followed by a partial etch into the cladding in a CHF_3/O_2 RIE step.

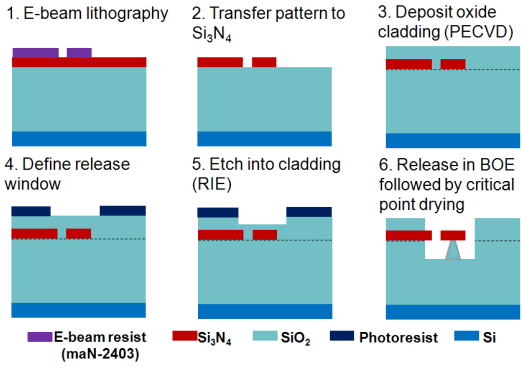

Figure 3: Illustration of process flow for micro-fabricating optomechanical components in silicon nitride

We then perform a timed release etch in buffered oxide etchant to undercut the devices, to enable opto-mechanics. The samples are then dried using a critical point dryer to prevent stiction. The resulting devices have cladding over the gratings, and the tapered section of the waveguide. Figure 4 shows an optical micrograph and a scanning electron micrograph (SEM) of the device.

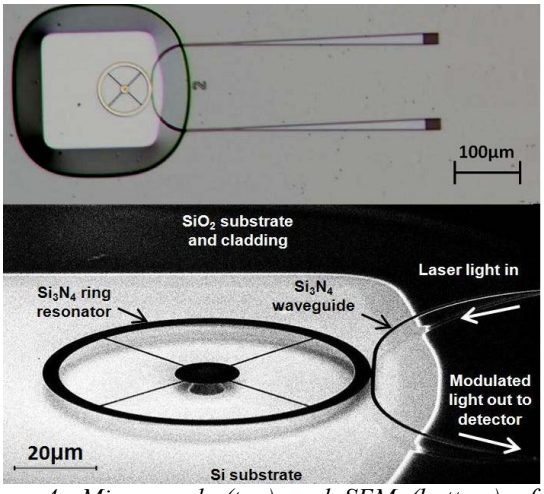

Figure 4: Micrograph (top) and SEM (bottom) of the device. The gap between the ring and waveguide at point of nearest approach is 50nm.

EXPERIMENTAL RESULTS

Optical characterization

We couple light from a tunable laser into the grating coupler and monitor the output using an optical power meter. The laser wavelength is swept to identify a high Q optical resonance. Figure 5 shows an optical resonance at 1550.474nm that has a total loaded optical quality factor

of 195,500 and an intrinsic optical Q > 500,000. The grating couplers introduce a loss of 8dB per coupler.

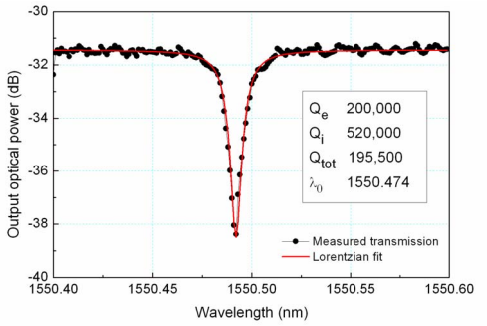

Figure 5: Optical spectrum showing the high-Q resonance. The input laser power was -15dBm.

Measurement of self-oscillations

We use the setup illustrated in Figure 6 to study the optomechanics in the silicon nitride OMO. We use an avalanche photodiode (APD) with a gain of 6,000V/W as the photodetector in our system. An Agilent E4445A spectrum analyzer is used to study the output RF spectrum and an Agilent E5052B signal source analyzer is used to measure phase noise of the oscillations.

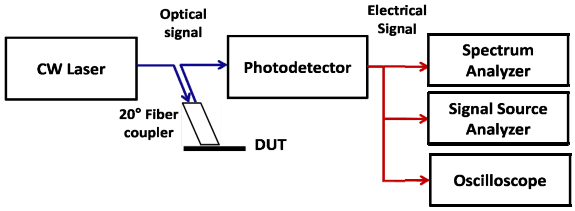

Figure 6: Schematic illustration of the test setup used to probe the mechanical resonance of the device

For high input laser power, the resonator heats up due to absorption, resulting in a characteristic shark fin optical spectrum as shown in Figure 7.

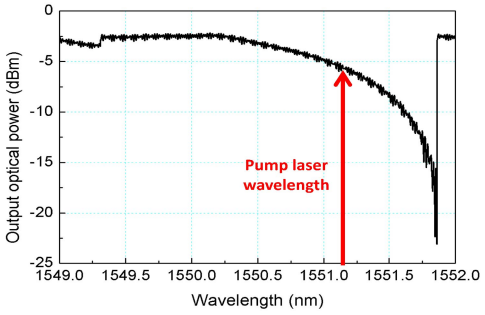

Figure 7: Shark fin optical resonance shape for 15dBm input laser power. The extinction at resonance is 20.2dB

This thermo-optical nonlinearity renders it difficult to detune the pump laser from the cavity resonance at the mechanical resonance frequency. In this situation, it is beneficial to fix the laser wavelength such that it corresponds to a 3dB drop in optical transmission, as shown in Figure 7. This results in sub-optimal amplification and hence increased optical threshold for self-oscillation [4], but with an improvement in extinction at the RF output (measured as the ratio of maximum voltage to minimum voltage for the RF output).

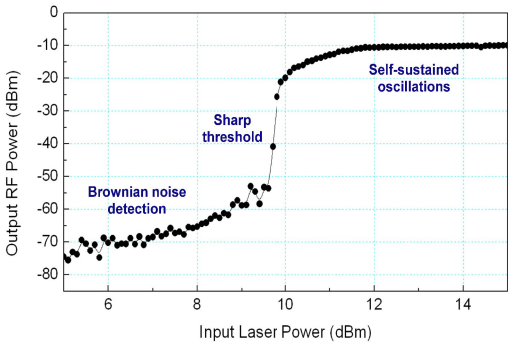

Figure 8: Radiation pressure induced parametric instability in the silicon nitride OMO.

Figure 8 shows the variation of RF output power at the photodetector with the input laser power. At low input laser powers, the input light coupled into the cavity is modulated by the Brownian noise motion of the fundamental radial expansion mode of the ring at 41.95MHz. The mechanical Q for this mode measured in air is 2,000. As we increase the laser power, self-sustained oscillations are observed above the input threshold power. The sharp threshold behavior is characteristic of radiation pressure induced parametric instability. Figure 9 shows measured RF output power above and below threshold.

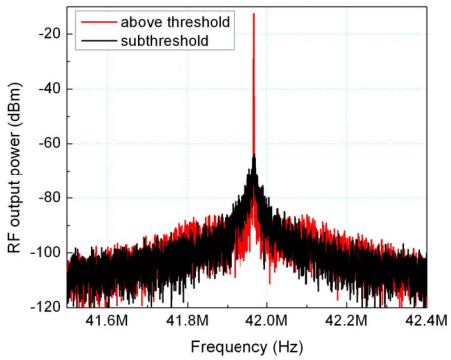

Figure 9:Measured RF output power for subthreshold (Brownian noise motion) and above threshold laser power (self-oscillation of the radial expansion mode)

The phase noise slope is -20dB/decade even down to 10Hz offset from carrier as shown in Figure 10. This implies that the RP-OMO has no flicker noise. This can be attributed to absence of an external amplifier and the integrated on-chip waveguide that eliminates coupling of low frequency environmental noise to the oscillator. The measured phase noise and threshold power match expected values as shown in Table 1. The threshold power is calculated at the waveguide, discounting the loss at the input grating coupler.

As shown in Figure 11, we achieve maximum extinction (defined as ratio of maximum output voltage to minimum output voltage at RF output of photodetector) for a laser wavelength that corresponds to 3dB drop in transmission. This corresponds to complete modulation of the optical mode shown in Figure 7.

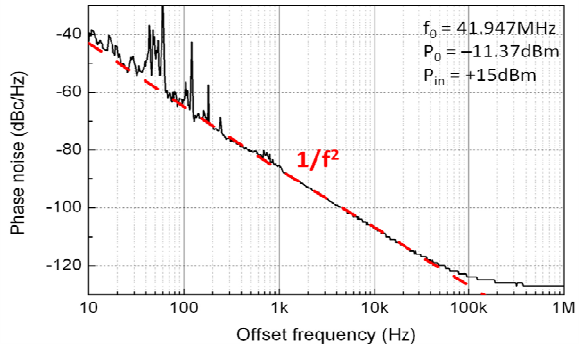

Figure 10: Phase noise for the silicon nitride RP-OMO with RF output signal power of -11.37dBm.

Table 1: Comparison of measured phase noise [10] and threshold power to expected simulated values.

	Measured	**Simulated**
Phase noise at 1kHz offset	-85dBc/Hz	-83dBc/Hz
Threshold power	3dBm	3.6dBm

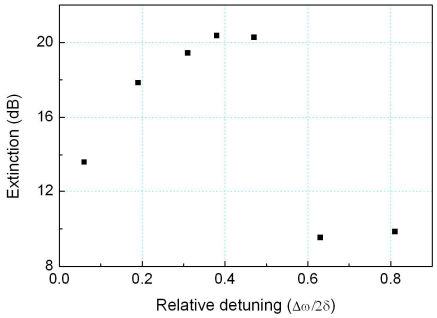

Figure 11: Extinction of oscillation waveform at output of the photodetector versus relative detuning (ratio of detuning to the resonance linewidth)

Improving phase noise of the OMO

Phase noise in OMOs depends strongly on optical quality factor [7]. Choosing a lower optical Q resonance while achieving complete modulation can give better phase noise at a cost of higher threshold power. We employed an optical mode with a total optical Q of 84,500 (and an intrinsic Q of 200,000) and observed a reduction in phase noise by 6dB as shown in Figure 12.

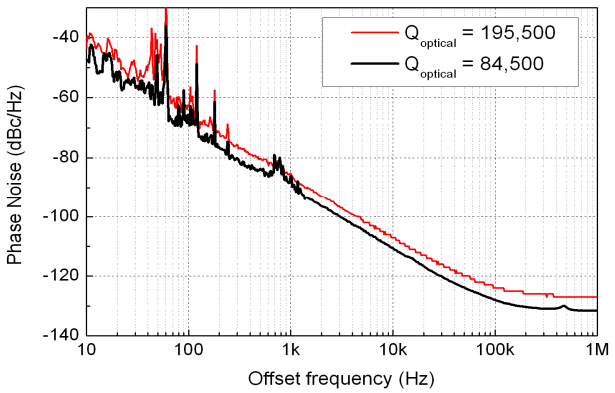

Figure 12: Improved phase noise for the RP-OMO using a lower optical Q resonance

CONCLUSION

We have presented a process flow for micro-fabricating integrated optomechanical components. Using these high optical Q resonators, we demonstrate an RP-OMO operating at 41.95MHz. This oscillator exhibits only $1/f^2$ phase noise and has promise as a long term stable oscillator for chip scale atomic clock (CSAC) and low bias drift oscillations for gyroscopes. We demonstrate the tradeoff between optical Q and laser power and improve the phase noise by 6dB achieving complete modulation of the pump laser light using a lower optical Q resonance.

ACKNOWLEDGEMENTS

The authors wish to thank David Hutchison for helping design the experimental setups. This work was supported by the DARPA ORCHID program and Intel Academic Research Office. The devices were fabricated at the Cornell NanoScale Science and Technology Facility.

REFERENCES

[1] W. -T. Hsu, and K. Cioffi, "Low Phase-Noise 70MHz Micromechanical Oscillators," *Digest IMS*, June 2004, pp. 1927-1930.

[2] H. M. Lavasani, F. Ayazi, et al., "A 145MHz low phase-noise capacitive silicon micromechanical oscillator," *IEEE IEDM*, Dec. 2008, pp. 1-4.

[3] C. Zuo, G. Piazza, et al., "1.05 GHz MEMS Oscillator Based On Lateral-Field-Excited Piezoelectric AlN Resonators," *IEEE IFCS*, April 2009, pp. 381-384.

[4] P. G. Steeneken, et al., "Piezoresistive heat engine and refrigerator," *Nature Physics 7*, 354–359 (2011).

[5] A. Rahafrooz, and S. Pourkamali, "High frequency dual-mode thermal-piezoresistive oscillators," *IEEE IFCS*, May 2011, pp. 1-4.

[6] T. J. Kippenberg and K. J. Vahala, "Cavity optomechanics: Back-action at the mesoscale," *Science* 29, 321 (5893), pp. 1172-1176, (2008).

[7] M. Hossein-Zadeh, K. J. Vahala, et al., "Characterization of a radiation-pressure-driven micromechanical oscillator," *Phys. Rev. A* 74, 023813 (2006).

[8] S. Tallur, et al., "Phase noise modeling of opto-mechanical oscillators," *IEEE IFCS*, June 2010, pp. 268-272.

[9] G. S. Wiederhecker, M. Lipson, et al., "Controlling photonic structures using optical forces," *Nature 462*, 633636 (2009).

[10] S. Tallur, et al., "A monolithic radiation-pressure driven, low phase noise silicon nitride opto-mechanical oscillator," *Optics Express 19*, 24522-24529 (2011).

CONTACT

*S. Tallur; sgt28@cornell.edu